A Fast Parallel Code for Calculating Energies and Oscillator Strengths of Many-Electron Atoms at Neutron Star Magnetic Field Strengths in Adiabatic Approximation

D. Engel [a], M. Klews [b], G. Wunner [a,1]

[a] *Institut für Theoretische Physik I, Universität Stuttgart, D-70550 Stuttgart, Germany*

[b] *Institut für Astronomie uud Astrophysik. Univ. Tübingen, Auf der Morgenstelle 9, D-72076 Tübingen, Germany*

Abstract

We have developed a new method for the fast computation of wavelengths and oscillator strengths for medium-Z atoms and ions, up to iron, at neutron star magnetic field strengths. The method is a parallelized Hartree-Fock approach in adiabatic approximation based on finite-element and B-spline techniques. It turns out that typically 15–20 finite elements are sufficient to calculate energies to within a relative accuracy of 10^{-5} in 4 or 5 iteration steps using B-splines of 6^{th} order, with parallelization speed-ups of 20 on a 26-processor machine. Results have been obtained for the energies of the ground states and excited levels and for the transition strengths of astrophysically relevant atoms and ions in the range $Z = 2 \ldots 26$ in different ionization stages.

PACS: 31.15.Ne, 32.60.+i, 95.30.Ky, 97.60.Jd

Key words: neutron star magnetic fields, atomic data, adiabatic approximation

PROGRAM SUMMARY

Manuscript Title: A Fast Parallel Code for Calculating Energies and Oscillator Strengths of Many-Electron Atoms at Neutron Star Magnetic Field Strengths in Adiabatic Approximation
Authors: D. Engel, M. Klews, G. Wunner,
Program Title: HFFEM
Journal Reference:

[1] Corresponding author

Catalogue identifier:
Licensing provisions: None
Programming language: Fortran 95 and Python
Computer: Cluster of 1–26 HP Compaq dc5750
Operating system: Fedora 7
RAM: 1 GByte
Number of processors used: 1–26
Keywords: neutron star magnetic fields, atomic data, adiabatic approximation, B-splines, finite elements
PACS: 31.15.-p, 31.15.Ne, 32.60.+i, 97.60.Jd
Classification: Atomic Physics, Structure and Properties
External routines/libraries: MPI/GFortran, LAPACK, PyLab/Matplotlib

Nature of problem:

Calculations of synthetic spectra [1] of strongly magnetized neutron stars are bedevilled by the lack of data for atoms in intense magnetic fields. While the behaviour of hydrogen and helium has been investigated in detail (see, e.g., [2]), complete and reliable data for heavier elements, in particular iron, are still missing. Since neutron stars are formed by the collapse of the iron cores of massive stars, it may be assumed that their atmospheres contain an iron plasma. Our objective is to fill the gap and to provide a program which allows users to calculate as comprehensively as possible energies, wavelengths, and oscillator strengths of medium-Z atoms and ions up to $Z = 26$ in neutron star magnetic field strengths. Obviously, the method for achieving this goal must be highly efficient since for the calculation of synthetic spectra data of many thousands or even millions of atomic transitions may be required.

Solution method:

As in previous work on the problem (cf. [3–7]) we exploit the fact that a strong magnetic field results in an approximate decoupling of the dynamics of the electrons parallel and perpendicular to the field. In this "adiabatic approximation" the single-particle wave functions take the form: $\psi_i(\rho, \varphi, z) = \phi_{nm}(\rho, \varphi) \cdot P_{nm\nu}(z)$, where $\phi_{nm}(\rho, \varphi)$ are Landau wave functions, describing the (fast) motion perpendicular to the field, and the $P_{nm\nu}(z)$ are the longitudinal wave functions, describing the (slow) bound motion along the direction of the field. The spins of the electrons are all aligned antiparallel to the magnetic field and need not be accounted for explicitly. The total N-electron wave function is constructed as a Slater determinant of the single-particle wave functions, and the unknown longitudinal wave functions are determined from the Hartree-Fock equations, which follow from inserting the total N-electron wave function into Schrödinger's variational principle for the total energy.

The novel feature of our approach [8] is to use finite-element and B-spline tech-

niques to solve the Hartree-Fock equations for atoms in strong magnetic fields. This is accomplished through the following steps: 1) decomposition of the z-axis into finite elements with quadratically widening element borders; 2) sixth-order B-spline expansion of the single-particle wave functions on the individual finite elements; 3) formulation of the variational principle equivalent to the Hartree-Fock equations in terms of the expansion coefficients. This leads to a simple system of linear equations for the expansion coefficients, which is solved numerically, and, since the direct and exchange interaction potential terms depend on the wave functions, in a self-consistent way. The iteration procedure is initialized by distributing the electrons on magnetic sublevels according to the level scheme of the hydrogen atom in intense magnetic fields.

To speed up the calculations, the code is parallelized. The parallelization strategy is: a) each processor calculates one or several electrons, depending on the total number of processors, b) single-particle wave functions are broadcast from each processor to every other processor. As the coefficient vectors in the B-spline basis are small (dim $\approx$ 20–25), there is only little communication between the nodes. Typical speed-ups by a factor of 20 are obtained on a 26-processor cluster of HP Compaq dc57750.

References:

[1] Werner, K., and Dreizler, S., "The Classical Stellar Atmosphere Problem" in *Computational Astrophysics,* edited by Riffert, H., Werner, K., *J. of Computational and Applied Mathematics*, Elsevier (1998).

[2] Ruder, H., Wunner, G., Herold, H., and Geyer, F., *Atoms in strong magnetic fields*, Springer, Heidelberg, (1994).

[3] Jones, P. B., *Mon. Not. R. Astron. Soc.* **216** (1985) 503.

[4] Neuhauser, D., Langanke, K., and Koonin, S. E., *Phys. Rev. A* **33** (1986) 2084.

[5] Miller, M. C., and Neuhauser, D., *Mon. Not. R. Astron. Soc.* **253** (1991) 107.

[6] Rajagopal, M., Romani, R. W., and Miller, M. C., *Astrophys. J.* **479** (1997) 347.

[7] Mori, K., and Hailey, C. J., *Astrophys. J.* **564** (2002) 914.

[8] Klews, M., "Discretization Methods for the Investigation of Atoms in Time-dependent Electric Fields, and in Extremely Strong Magnetic Fields," *Doctoral Thesis*, University of Tübingen, (in German), (2003). http://www.theo1.physik.uni-stuttgart.de/forschung/sfb382a15/klews_2003.ps.gz

LONG WRITE-UP

1 Introduction

Thermal emission of isolated neutron stars with strong cosmic magnetic fields (10^6 to 10^9 T) and temperatures of several 10^5 K was first observed by the ROSAT satellite in the soft X-ray band (see, e.g., Zampieri et al. [1] for the complete list of the sources discovered). More recently, and with higher accuracy, thermal spectra of isolated neutron stars have been measured using the X-ray satellites Chandra and XMM Newton. The observation of features in the X-ray spectra of the neutron star 1E 1207 [2,3] and three other isolated neutron stars [4–6] has rekindled the interest in the calculation of atomic data of medium-heavy elements in neutron star magnetic fields, up to the last fusion product element iron, since the observed features could have an atomic origin. The features could provide important information on the chemical composition of the neutron star surface, the surface gravity from the line broadening, the mass-to-radius ration from the gravitational redshift of the lines, and the strength of the surface magnetic field.

However, quantitative analyses of these spectra by means of model atmosphere calculations are still greatly handicapped by the lack of sufficiently complete and accurate sets of atomic data at such huge magnetic field strengths. While for hydrogen and helium many and accurate results for energy levels and transition rates have been obtained (see, e.g., [7–12]), for $Z > 2$ atomic data are available to a much lesser extent. Calculations are much harder since the problem of solving the many-electron Schrödinger equation is aggravated by the fact that the magnetic-field effects must be considered non-perturbatively. At neutron star magnetic field strengths the magnetic field effects are of the same order or even larger than those of the Coulomb field, angular momentum is no longer a good quantum number, and the familar atomic shell structure has completely collapsed. Different methods have been used in the literature to tackle the problem, ranging from rigorous mathematical estimates over density-functional and discrete-variable methods to different self-consistent field approaches [13–47].

In this paper we will apply the Hartree-Fock method in adiabatic approximation to the problem of heavy atoms and ions in neutron star magnetic fields. This approximation is justified when the neutron star magnetic field strength well exceeds the reference magnetic field strength B_Z for nuclear charge Z, $B_Z = Z^2\,B_0$, with $B_0 = 4.70108 \times 10^5$ T. The reference magnetic field strength marks the transition from Coulomb field dominance to magnetic field dominance, since at B_Z the Larmor radius $a_{\rm L} = \sqrt{2\hbar/(eB)}$ becomes equal to the nuclear-charge scaled Bohr radius $a_Z = a_0/Z$. At B_Z, the cyclotron en-

ergy $\hbar\omega_C = \hbar eB/m$ is four times the Rydberg energy for nuclear charge Z, $E_Z = Z^2 E_{\rm Ryd}$, and thus the effects of the magnetic field and the Coulomb atrraction are of the same order of magnitude.

The advantage of using the adiabatic approximation is that energies, wave functions and oscillator strengths can be computed fast and in a routine way, which is a prerequisite for generating the amount of atomic data required by astronomers for the calculation of synthetic spectra. Moreover, even at magnetic field strengths where the adiabatic approximation becomes poor ($B \sim Z^2 B_0$) these values still provide valuable estimates for the correct energies and oscillator strengths. In addition, the wave functions can be used to initialize more sophisticated methods which go beyond the adiabatic approximation, such as Hartree-Fock-Roothaan calculations [48,49], or serve as guiding wave functions in quantum Monte Carlo simulations of heavy atoms and ions in strong magnetic fields [50].

Hartree-Fock calculations for many-electron atoms in adiabatic approximation have been performed by Neuhauser et al. [41], Miller and Neuhauser [42], and Rajagopal et al. [43]. Our approach which is based on the work of Klews [51] improves on their calculations by the use of more advanced and efficient numerical techniques, viz. finite elements and B-spline interpolation [52,53]. Furthermore, we have implemented the method in a parallelized fashion and written a code which can be handed over to and applied by the public user.

2 Hartree-Fock equations in adiabatic approximation

2.1 Adiabatic approximation

The adiabatic approximation proposed by Schiff and Snyder [54] assumes a decoupling between the motions of the electrons parallel and perpendicular to the field. This is the case if, in classical terms, the gyration of the electron in the plane perpendicular to the field is fast in comparison with the motion along the field direction, which is caused by the Coulomb interaction with the positively charged nucleus or core. Quantitatively, this requires the typical length scale of the gyration, the Larmor radius, to be much smaller than the typical Coulomb binding length, the Bohr radius for charge Z, $a_{\rm L} \ll a_Z$, which implies for the dimensionless magnetic field parameter $\beta_Z \equiv B/B_Z \gg 1$. In quantum terms, the decoupling amounts to a product form of the single-particle orbitals from which Slater determinants of the N-electron atoms or ions are constructed. Each single-particle orbital ψ_i is a product of a Landau

state $\phi_{n,m}$ and a longitudinal wave functions $P_{n,m,\nu}$

$$\psi_i(\vec{r}) = \phi_{nm}(\rho,\varphi)\ P_{nm\nu}(z)\,. \tag{1}$$

In (1) n denotes the Landau level ($n = 0, 1, 2, \dots$), m is the magnetic quantum number ($m = n, n-1, n-2, \dots$), and ν is the number of nodes of the longitudinal wave function. The Landau states $\phi_{n,m}$ are the analytical eigensolutions of the Schrödinger equation of an electron in a magnetic field with energies $E_n = n\hbar\omega_{\rm C}$. For $B \geq 10^7$ T the cylotron energy $\hbar\omega_C \geq 1$ keV. Since the single-particle Coulomb excitation energies turn out to be much smaller than $\hbar\omega_C$, it is not necessary to include excited Landau states, and one can restrict oneself to the lowest Landau level, $n = 0$. In this level, all electrons have spin down, and therefore the spin quantum number can be omitted in what follows.

The longitudinal wave functions are then determined by solving the Hartree-Fock equations

$$\begin{aligned}\Big[-\frac{\mathrm{d}^2}{\mathrm{d}z^2} + V_i^{\rm EF}(z) - \epsilon_i + \sum_{j\neq i}\int P_j(z')P_j(z')W_{ij}^{\rm DI}(z,z')\,\mathrm{d}z'\Big]P_i(z)& \\ = \sum_{j\neq i} P_j(z)\int P_j(z')P_i(z')W_{ij}^{\rm EX}(z,z')\,\mathrm{d}z'\ ,&\end{aligned} \tag{2}$$

with the three functions $V_i^{\rm EF}(z)$, $W_{ij}^{\rm DI}(z,z')$, and $W_{ij}^{\rm EX}(z,z')$ for the effective electron-nucleus potential, the direct electron-electron potential, and the electron-electron exchange potential, respectively:

$$V_i^{\rm EF}(z) = -2Z\int \frac{\phi^*_{0m_i}(\rho,\varphi)\phi_{0m_i}(\rho,\varphi)}{|\vec{r}|}\,\mathrm{d}r_\perp\,, \tag{3}$$

$$W_{ij}^{\rm DI}(z,z') = 2\iint \frac{\phi^*_{0m_i}(\rho,\varphi)\phi_{0m_i}(\rho,\varphi)\phi^*_{0m_j}(\rho',\varphi')\phi_{0m_j}(\rho',\varphi')}{|\vec{r}-\vec{r}'|}\mathrm{d}r_\perp\,\mathrm{d}r'_\perp, \tag{4}$$

$$W_{ij}^{\rm EX}(z,z') = 2\iint \frac{\phi^*_{0m_i}(\rho,\varphi)\phi_{0m_i}(\rho',\varphi')\phi^*_{0m_j}(\rho',\varphi')\phi_{0m_j}(\rho,\varphi)}{|\vec{r}-\vec{r}'|}\mathrm{d}r_\perp\mathrm{d}r'_\perp. \tag{5}$$

It is well known (see. e.g., Fig. 20 in Canuto and Ventura [55]) that the spectrum of the hydrogen atom in a strong magnetic field decomposes into a group of tightly bound states (one for each magnetic quantum number m), which for small magnetic quantum numbers are separated by a large energy gap (on the order of 100 eV) from the remaining states. The latter have been labelled hydrogen-like states since in the limit $B \to \infty$ they converge to a Rydberg series. With this single-electron spectrum in mind it is reasonable to construct Slater determinants for low-lying states of the N-electron problem by placing

electrons successively into the tightly bound states with $m = 0, -1, -2, \ldots$, until for some value of m the energy of the tighly bound state intrudes into the hydrogen-like part of the spectrum, and electrons have to be placed in hydrogen-like states with low absolute values of m.

2.2 Solution of the Hartree-Fock equations using finite elements and B Splines

In the theory of finite elements (see, e.g., [56,57]) the domain $\Omega \subseteq R^n$, on which a variational principle $\Pi = \int_\Omega d\Omega\, F(f(\vec{r})) = \text{extr.}$ is defined, is divided into subdomains Ω_i, with $\bigcup_i \Omega_i = \Omega$, so that the functional becomes a sum over these finite elements, $\Pi = \sum_i \int_{\Omega_i} F(f(\vec{r}))$. In each element, specified by the index i, the function f is approximated by local basis functions $P_k^{(i)}$, with expansion coefficients $\phi_k^{(i)}$, $f^{(i)} = \sum_k \phi_k^{(i)} P_k^{(i)}$, and the variation with respect to the coefficients leads to an algebraic system of equations $\partial\Pi/\partial\vec{\phi} = 0$, where $\vec{\phi}$ is the vector formed by all expansion coefficients on all the finite elements. For a system of linear differential equations

$$\hat{A}\vec{f} + \vec{b} = 0, \tag{6}$$

with a self-adjoint operator $\hat{A}$, the associated functional is (e.g. [56])

$$\Pi = \int_\Omega (\vec{f}^{\,T}\, \hat{A}\vec{f} + 2\vec{f}^{\,T}\, \vec{b})\, d\Omega\,, \tag{7}$$

and the variational principle leads to a *linear* system of equations for the expansion coefficients,

$$\partial\Pi/\partial\vec{\phi} = L\vec{\phi} + \vec{c} = 0\,, \tag{8}$$

with a symmetric banded matrix L.

The Hartree-Fock equations (2) are of the type (6), and therefore the above concepts can be applied to their solution. The situation is particularly simple as the domain is one-dimensional, and thus the finite elements become subintervals of the z axis. Since the wave functions exponentially decay at large z the domain can be bounded by some maximum value $z_{\max}$. The interval $[0, z_{\max}]$ is divided into n finite elements with quadratically widening element borders ($z_i = (i-1)^2\, z_{\max}/n^2,\ \ i = 1, \cdots, n+1$). The quadratic widening accounts for the decay of the wave functions further away from the nucleus. Other partition schemes such as cubic or exponential widening of the element borders are also implemented in the code as options.

As local basis functions on the finite elements we use B-splines, i.e. the longitudinal part of each single-particle orbital $\psi_i(\vec{r}) \equiv \phi_i(\rho, \varphi)\ P_i(z)$ is approximated by

$$P_i(z) = \sum_l \alpha_l^{(i)} B_l(z). \tag{9}$$

Given a node sequence $\{z_i\}$, with $z_{i+1} \geq z_i$, B-splines of order k are defined recursively via (cf. [52,53])

$$B_{i,k}(z) = \frac{z - z_i}{z_{i+k-1} - z_i} B_{i,k-1}(z) + \frac{z_{i+k} - z}{z_{i+k} - z_{i+1}} B_{i+1,k-1}(z) \tag{10}$$

$$B_{i,1}(z) = \begin{cases} 1, & z_i < z < z_{i+1} \\ 0, & \text{otherwise} \end{cases} . \tag{11}$$

They are polynomials of degree $k-1$ and add up to unity on the interpolation interval. The node sequence of the splines is given by the borders of the finite elements inside the interpolation interval, the edges of the interpolation interval have to considered as k multiple nodes to guarantee that the B-splines are $(k-2)$ times continuously differentiable over the interpolation interval. Fig. 1 shows an example of a quadratic ($k = 3$) B-spline basis set for quadratically widening element borders over the interval $[0, 36]$.

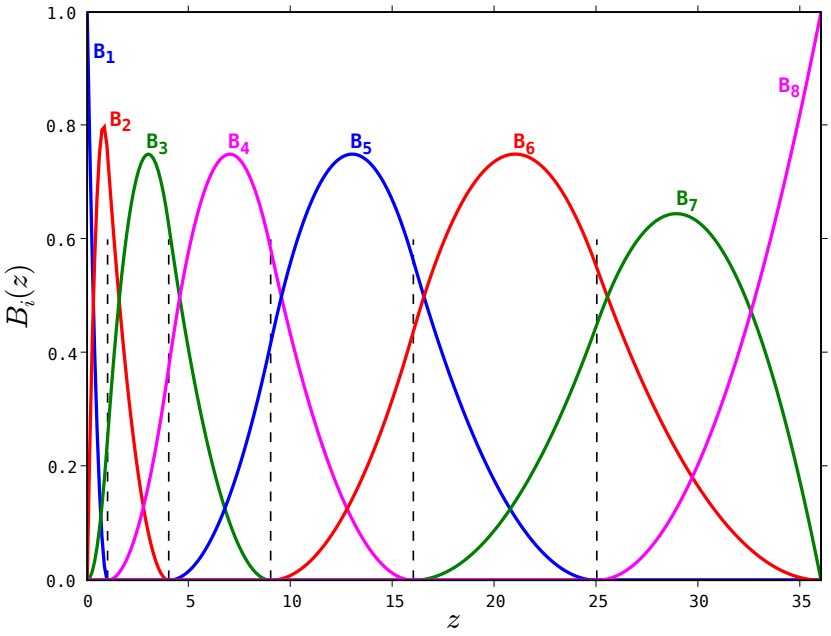

Fig. 1. Complete quadratic ($k = 3$) B-spline basis sets for interpolation in the interval $[0, 36]$ with quadratically widening element borders. The borders of the interpolation interval are triple nodes.

The self-consistent solution of the Hartree-Fock equations (2) now means determining the expansion coefficients $\alpha_l^{(i)}$ for the N single-electron orbitals $P_i(z)$. According to (7) the functional associated with the Hartree-Fock equa-

tions is given by

$$\Pi = \int_{-\infty}^{\infty} \Big(P_i(z) \hat{A} P_i(z) + 2 P_i(z) b(z) \Big) \, \mathrm{d}z \tag{12}$$

with the operators

$$\hat{A} = \frac{\mathrm{d}^2}{\mathrm{d}z^2} - V_i^{\mathrm{EF}}(z) + \epsilon_i - \sum_{\substack{j=1 \\ j \neq i}}^{N} \int_{-\infty}^{\infty} P_j^2(z') W_{ij}^{\mathrm{DI}}(z, z') \, \mathrm{d}z', \tag{13}$$

$$b(z) = \sum_{\substack{i,j=1 \\ i \neq j}}^{N} P_j(z) \int_{-\infty}^{\infty} P_j(z') P_i(z') W_{ij}^{\mathrm{EX}}(z, z') \, \mathrm{d}z'. \tag{14}$$

Of course, with (12) we recover the original energy functional.

The system of inhomogeneous linear equations corresponding to (8) now reads

$$\sum_{j,l} A_{kl}^{(j)} \alpha_l^{(i)} = - \sum_j b_k^{(j)} \ . \tag{15}$$

For a given single-particle orbital P_i the matrix $A_{kl}^{(j)}$ and the vector $b_k^{(j)}$ are determined by

$$A_{kl}^{(j)} = \int_0^{z_{\max}^{(j)}} B_k(z^{(j)}) \, \hat{A} \, B_l(z^{(j)}) \, \mathrm{d}z^{(j)} \ , \tag{16}$$

$$b_k^{(j)} = \int_0^{z_{\max}^{(j)}} B_k(z^{(j)}) \, b(z^{(j)}) \, \mathrm{d}z^{(j)} \ , \tag{17}$$

where $z^{(j)}$ is the local variable on the jth finite element. Since the effective potentials appearing in the definition of the operators $\hat{A}$ and b depend on the longitudinal wave functions, and thus on the coefficients, the solution of the system of linear equations (15) has to be found iteratively in a self-consistent way.

Our calculations were performed using B-splines of order $k = 6$ and typically 15–20 finite elements. For the states considered the outer boundary of the interval was in the range $z_{\max} \sim 2 - 30$ atomic units. Depending on the many-electron state it was chosen in such a way that all single-particle orbitals have decayed to zero exponentially.

2.3 Choice of initial wave functions

The iteration is initialized by distributing the electrons on magnetic sublevels according to the level scheme of the hydrogen atom in intense magnetic fields.

As initial wave functions we choose the approximate solutions for the hydrogen atom in a strong magnetic field according to Canuto and Kelly [58] which can be expressed in analytical form. Their expansion coefficients in the B-spline basis are obtained in a standard way by solving the system of inhomogeneous linear equations which follow from the interpolation problem with complete boundary conditions.

2.3.1 Tightly bound states

The approximate analytical solutions for the tightly bound states according to Canuto and Kelly [58] are given by

$$P_m(z) \sim \exp\left(-\frac{\lambda_m^2}{2}\frac{z^2}{a_{\mathrm{L}}^2}\right), \tag{18}$$

where the variational parameter λ_m is determined from

$$\lambda_m = \frac{4\,a_{\mathrm{L}}}{a_0\sqrt{\pi}}\left[\ln\left(\frac{2}{\lambda_m}\right) - 1 - \frac{1}{2}A_m\right] \tag{19}$$
$$\text{with} \quad A_0 := 0 \quad \text{and} \quad A_m := \sum_{k=1}^{-m}\frac{1}{k} \quad \text{for} \quad m \le -1.$$

The transcendental equation is solved numerically in the code by the Brent method [59].

2.3.2 Hydrogenlike states

Approximate analytical solutions for the hydrogen-like states according to Canuto and Kelly [58] can be obtained by a perturbation theory approach. The actual effective potentials $V_m(z)$ calculated by averaging the electron-nucleus interaction over the Landau state $\phi_{0m}(\vec{r}_\perp)$ are replaced with one-dimensional truncated Coulomb potentials $V_m \propto 1/(|z|+d_m)$, with a truncation parameter d_m, and their difference is treated as a perturbation. For excited states in the truncated potentials, with quantum numbers $(m \le 0, \nu > 0)$, the analytical eigensolutions read

$$P_m(z) \sim W_{\alpha,\frac{1}{2}}(\zeta) \quad \text{with} \quad \zeta := \frac{2z}{\alpha_m a_0} + \frac{2d_m}{\alpha_m a_0}\,, \tag{20}$$

where $W_{\alpha,\frac{1}{2}}$ are Whittaker functions, and the parameters d_m and α_m follow from the condition that the expectation values of the exact Coulomb potential and the truncated Coulomb potential conincide.

For excited states with negative z parity (odd number of nodes) the result is

[58]

$$\alpha_m^{\rm odd} = p + \frac{2\,d_m^{\rm odd}}{a_0}\,, \quad \text{with} \quad p = 1, 2, \ldots \quad (\nu = 2p-1)\,, \tag{21}$$

$$d_m^{\rm odd} = \frac{p\,a_0}{\lambda_m}\,[\ln(\lambda_m) - 1]\,, \quad \text{with} \quad \lambda_m = \frac{4\,p^2 a_0^2}{(1-m)\,a_{\rm L}^2}\,. \tag{22}$$

For excited states with positive z parity (even number of nodes) the result is [58]

$$\alpha_m^{\rm even} = p + \frac{1}{t_m + \sqrt{t_m^2 + \frac{\pi^2}{3}}}\,, \quad \text{with} \quad p = 1, 2, \ldots \quad (\nu = 2p)\,, \tag{23}$$

$$\text{and} \quad t_m = -0.58 - \frac{d_m^{\rm even}}{a_0} - \frac{1}{2}\ln\left(\frac{2\,d_m^{\rm even}}{a_0}\right) + \frac{1}{24p^2}\,,$$

$$d_m^{\rm even} = \sqrt{\frac{1-m}{\gamma}}\,\frac{a_{\rm L}}{2}\,, \tag{24}$$

where in the last equation $\gamma \approx 0.577$ is the Euler-Mascheroni constant. The Whittaker functions can be expressed in terms of confluent hypergeometric functions which in the code are evaluated using the algorithm of [60].

2.4 Calculation of the effective potentials

The calculation exploits the Laplace transform of the Coulomb potential in cylindrical coordinates

$$\frac{1}{\sqrt{\rho^2 + z^2}} = \int_0^\infty \mathrm{e}^{-kz} J_0(k\rho)\,\mathrm{d}k\,, \tag{25}$$

where J_0 designates the ordinary Bessel function of order 0. Calculating the expectation value of (25) with respect to the Landau state

$$\phi_{n,m=n-s}(\rho,\varphi) = \pi^{-1/2}\mathrm{e}^{i(n-s)\varphi} I_{n,s}(\rho^2)\,, \tag{26}$$

with the generalized Laguerre functions $I_{n,s}$ (cf. Sokolov and Ternov [61], or Canuto and Ventura [55]), and using the general expression [61]

$$\int_0^\infty I_{\alpha\beta}(x) I_{\gamma\sigma}(x) J_{\alpha-\beta-\gamma+\sigma}\left(2\sqrt{Ax}\right)\,\mathrm{d}x = I_{\alpha\gamma}(A) I_{\beta\sigma}(A) \tag{27}$$

one obtains, for states in the lowest Landau level with magnetic quantum number m_i, the effective electron-nucleus potential (3)

$$V_i^{\rm EF}(z) = -\frac{2Z}{(-m_i)!}\sqrt{\beta}\int_0^\infty \exp\left(-\sqrt{\beta}zy - \frac{y^2}{4}\right) L_{-m_i}^0\left(\frac{y^2}{4}\right)\mathrm{d}y\,, \tag{28}$$

where L_k^q are the generalized Laguerre polynomials. Equation (28) can be evaluated in a standard manner by Gauss-Laguerre quadrature.

The calculation of the direct and exchange potentials exploits the more general expansion of the Coulomb interaction in terms of ordinary Bessel functions

$$\frac{1}{|\vec{r}_1 - \vec{r}_2|} = \int_0^\infty \mathrm{e}^{-k|z_1 - z_2|} \sum_{m=-\infty}^{m=+\infty} \mathrm{e}^{im|\varphi_1 - \varphi_2|} J_m(k\rho_1) J_m(k\rho_2)\, \mathrm{d}k\,, \qquad (29)$$

and with the help of (27) one finds for states in the lowest Landau level with magnetic quantum numbers m_i, m_j

$$W_{ij}^{\mathrm{DI}}(z, z') = \frac{2\sqrt{\beta}}{|m_i|!|m_j|!} \int_0^\infty \mathrm{e}^{\left(-\sqrt{\beta}|z_i - z_j| y - \frac{y^2}{4}\right)} L_{-m_i}^0(\frac{y^2}{4}) L_{-m_j}^0(\frac{y^2}{4})\, \mathrm{d}y\,, \qquad (30)$$

$$W_{ij}^{\mathrm{EX}}(z, z') = \frac{2\sqrt{\beta}}{|m_i|!|m_j|!} \int_0^\infty \mathrm{e}^{\left(-\sqrt{\beta}|z_i - z_j| y - \frac{y^2}{4}\right)} \left(\frac{y^2}{4}\right)^{m_i - m_j} \left[L_{-m_i}^{m_i - m_j}(\frac{y^2}{4})\right]^2 \mathrm{d}y\,. \qquad (31)$$

Again these expressions can be evaluated by standard Gauss-Laguerre quadratures.

2.5 Oscillator strengths

The matrix element (in atomic units) of a $\Delta M = q$ dipole transition between two states Ψ and Ψ' is defined by

$$p_{\Psi'\Psi}^{(q)} = \langle \Psi' | \sum_{j=1}^{N} \hat{r}_j^{(q)} \, | \Psi \rangle \,, \qquad (32)$$

where $\hat{r}_i^{(q)}$ are the spherical components of the position operator. The modulus squared of (32) is called the dipole strength of the transition,

$$d_{\Psi'\Psi}^{(q)} = |p_{\Psi'\Psi}^{(q)}|^2 \,, \qquad (33)$$

which when multiplied by the energy difference (in Rydberg units) of the two states yields the oscillator strength of the transition

$$f_{\Psi'\Psi}^{(q)} = (E_{\Psi'} - E_\Psi)\, d_{\Psi'\Psi}^{(q)} \,. \qquad (34)$$

As is well known, if the N-electron states Ψ and Ψ' are given as Slater determinants, with single-electron orbitals ψ_i and ψ_i', respectively, the matrix element (32) can be expressed in terms of matrix elements of the different

single-electron states,

$$p^{(q)}_{\Psi'\Psi} = \langle\Psi'|\sum_{j=1}^{N}\hat{r}_j^{(q)}\,|\Psi\rangle = \det(\mathcal{S}^{\Psi'\Psi})\sum_{i,j=1}^{N}\langle\psi'_i|\hat{r}_j^{(q)}|\psi_j\rangle\,(\mathcal{T}^{\Psi'\Psi})_{ij}. \tag{35}$$

Here $\mathcal{S}^{\Psi'\Psi}$ is the overlap matrix of the single-electron states

$$(\mathcal{S}^{\Psi'\Psi})_{i,j} := \langle\psi'_i|\psi_j\rangle\ , \tag{36}$$

and $\mathcal{T}^{\Psi'\Psi}$ is the transpose of its inverse

$$\mathcal{T}^{\Psi'\Psi} := ((\mathcal{S}^{\Psi'\Psi})^{-1})^{\mathrm{T}}. \tag{37}$$

In adiabatic approximation with all electrons in the lowest Landau level and with single-electron longitudinal wave functions $P'_{m'_i\nu'_i}(z)$ for the final and $P_{m_j\nu_j}(z)$ for the initial state the elements of the overlap matrix are simply given by:

$$\langle\psi'_i|\psi_j\rangle = \delta_{m'_i m_j}\,\langle P'_{m'_i\nu'_i}|P_{m_j\nu_j}\rangle \tag{38}$$

because of the orthogonality of the Landau states with different m.

For the different polarizations of the dipole transitions ($\Delta M = 0$ linear, $\Delta M = \pm 1$ circular) one obtains for the single-electron dipole matrix elements:

$$\begin{aligned}
\langle\psi'_i|\hat{r}^{(0)}|\psi_j\rangle &= \quad\delta_{m'_i m_j}\,\langle P'_{m'_i\nu'_i}|\,z\,|P_{m_j\nu_j}\rangle\ ,\\
\langle\psi'_i|\hat{r}^{(+1)}|\psi_j\rangle &= -\delta_{m'_i(m_j+1)}\,\langle P'_{m'_i\nu'_i}|P_{m_j\nu_j}\rangle\,\sqrt{|m_j|}/\sqrt{2\beta}\ ,\\
\langle\psi'_i|\hat{r}^{(-1)}|\psi_j\rangle &= \quad\delta_{m'_i(m_j-1)}\,\langle P'_{m'_i\nu'_i}|P_{m_j\nu_j}\rangle\,\sqrt{|m'_i|}/\sqrt{2\beta}\ .
\end{aligned} \tag{39}$$

Inserting these results into (35) yields the dipole matrix elements and via (34) the oscillator strengths in adiabatic approximations computed by the code.

2.6 Results and accuracies

Numerical results obtained using the present HFFEM code have been published in Refs. [49,50] where they are compared with the results of more advanced (but slower) methods as a function of magnetic field strength and nuclear charge.

In Ref. [50] the HFFEM wave functions, augmented by a Jastrow factor, served as guiding wave functions for released-phase diffusion quantum Monte Carlo (RPDQMC) calculations of ground states of atoms and ions in strong magnetic fields. The RPDQMC values are the most accurate results for ground state energies in the literatue to date. The comparison of the HFFEM energy values with the RPDQMC energy values in the Tables I – IV of Ref. [50] shows the

following deviations:
for $B = 10^7$ T: ranging from 3.3 per cent for helium, 8.7 per cent for carbon, to 13.6 per cent for neon;
for $B = 5 \times 10^7$ T: ranging from 1.6 per cent for helium, 3.4 per cent for carbon, 5.1 per cent for neon to 6.7 per cent for silicon;
for $B = 10^8$ T: ranging from 1.3 per cent for helium, 2.4 per cent for carbon, 3.4 per cent for neon, 4.3 per cent for silicon, 5.8 per cent for calcium, to 7.1 per cent for iron ;
$B = 5 \times 10^8$ T: ranging from 0.8 per cent for helium, 1.1 per cent for carbon, 1.4 per cent for neon, 1.8 per cent for silicon, 2.3 per cent for calcium, to 2.7 per cent for iron.
The reason why the deviations become smaller as the magnetic field increases is of course that the adiabatic approximation becomes more and more justified. The comparison of the ground state energies of iron ions at $B = 5 \times 10^8$ T in Table V of Ref. [50] shows deviations of 7.3 per cent for helium-like, 4.2 per cent for carbon-like, 3.4 per cent for neon-like, down to 2.7 per cent for neutral iron.

In Ref. [49] the HFFEM wave functions were used to initialize a multi-configurational Hartree-Fock approach in which up to 8 Landau levels were taken into account. That method also allows for the calculation of excited states and oscillator strengths. The comparison of oscillator strenghts of transitions to the carbon ground state in Table V of Ref. [49] and of transitions to the ground states of iron ions in Table VI shows that the improvements are large only for transitions with very small oscillator strengths, while for large oscillator strengths taking into account more Landau levels does not significantly change the values calculated in adiabatic approximation. Thus it may be concluded that the energies and oscillator strengths calculated using the HFFEM code already well reproduce the general features of the exact level scheme.

3 Program description

3.1 Program structure

The HFFEM code is written in Fortran 95 using MPI for parallelization. Apart from MPI, a LAPACK library for elementary linear algebra operations is needed. For the calculation of B-splines and confluent hypergeometric functions programs are included (bspline.f, mchgu.f) that are publicly available, and their origins are given in the headers of the source codes [52,60].

The program calculates one or two atomic states, and if a second state is to be calculated it additionally computes the oscillator strength. HFFEM runs

through the following stages 1–7 to calculate two atomic states. If only one single state is calculated the stages 5–7 are skipped.

(1) Read initial job parameters
(2) Distribute electrons over available MPI processes
(3) Call main iteration loop `HFITER` for the first state
(4) Write results of the first state
(5) Call main iteration loop `HFITER` for the second state
(6) Write results of the second state
(7) Calculate oscillator strength

The following parallelization strategy was implemented: In stages (3) and (5) the computation of the single-particle wave functions can be executed parallelly. Thus, in a typical program run, each electron is computed by a single MPI process on a distinct processor core. After every iteration step the wave functions (i. e. the B-spline expansion coefficients) are broadcast to the other processes. This parallelization strategy leads to a speed-up of 20 for the calculation of the neutral iron ground state on a 26-processor machine, with a run time of ~ 100 seconds.

The initial job parameters of the HFFEM program are:

`job:` name of the job
`natom:` number of electrons
`fm:` number of finite elements
`zatom:` atomic number
`bfield:` magnetic fields strength in Tesla
`zmax:` maximum value of the longitudinal z coordinate
`calcnum:` number of states to be calculated (1 or 2)
`fempart:` partition type of the finite elements (0: quadratic, 1: cubic, 2: quadratic-linear)

After these parameters are read via Fortran 95 namelist I/O, in a second step the quantum numbers $(-m, \nu)$ and the free parameter a for the initial wave functions are read line by line for each electron. The computation of the initial wave functions is done by setting the Larmor radius to the fixed value $a_{\mathrm{L}} = 1/\sqrt{\beta}$ and the Bohr radius is considered a free parameter $a_0 = a$. A zero input value for a means that the program chooses its default value. The default value is $a = 1.0$ for hydrogenlike states ($\nu > 0$) and $a = 1/Z$ for tightly bound states ($\nu = 0$).

Additionally, the HFFEM code generates for each calculated state a data file (file name extension `DAT`), a plot file containing the wave functions of the initial 4 iterations (file name extension `IPL`), and another plot file that contains the wave functions of the final iteration (file name extension `FPL`).

The number of MPI processes is determined at run time. If there are more MPI processes than electrons, the additional processes are idle and do not improve the performance. If there are fewer MPI processes than electrons, some processes compute more than one electron wave function.

The program package submitted along with this paper contains input files for three elements, viz. helium, carbon, and iron. For simplicity we explain the use of the program for the lightest element, and for reasons of space we here provide test run outputs only for helium and carbon.

The following sample input file `HE1011.INI` computes two helium states at $B = 9.40216 \times 10^7$ T ($\beta_Z = 50$) with quantum number (m, ν) set to $(0, 0)$ and $(-1, 0)$ for one state, and to $(0, 0)$ and $(-1, 1)$ for the other state.

```
&para job='HE1011',natom=2,fm=15,zatom=2,
bfield=94021600.0,zmax=8.d0,calcnum=2,fempart=2/
0 0 0.0
1 0 0.0
0 0 0.0
1 1 0.0
```

To run the program in two MPI processes on the present machine the HFFEM code is executed by `mpirun`:

```
mpirun -np 2 ./hffem < HE1011.INI
```

In order to plot the `IPL` and `FPL` files, the auxiliary PyLab Python scripts `iplot` and `fplot` can be used. For example, to plot the final wave functions of the second state (base name extension `-2ND`) of `HE1011` the `fplot` script is called:

```
./fplot HE1011-2ND
```

The sample output of the Python script is shown in Fig. 2 for an excited helium state and in Fig. 3 for an excited carbon state.

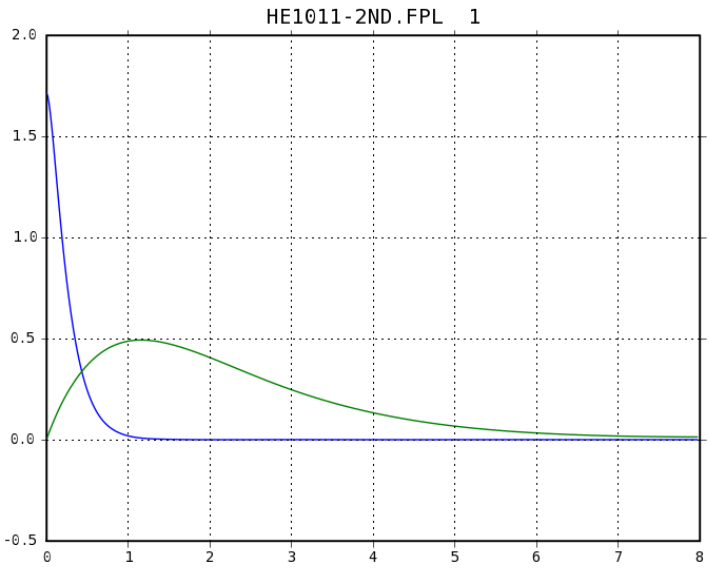

Fig. 2. Final longitudinal wave functions of the excited state of the helium example job `HE1011`. It is generated by the PyLab Python script `fplot`. The data stem from the plot file `HE1011-2ND.FPL`.

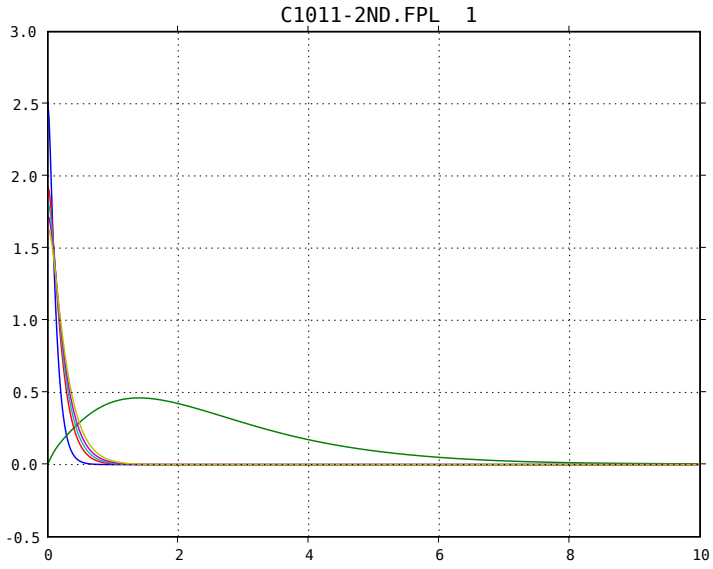

Fig. 3. Final longitudinal wave functions of the excited state of the carbon example job `C1011`. It is generated by the PyLab Python script `fplot`. The data stem from the plot file `C1011-2ND.FPL`.

TEST RUN OUTPUT OF HE1011.INI

```
STARTING HFFEM IN  2 MPI PROCESSES: 2008-02-06 15:43:20.242 +0100

PARAMETERS OF JOB HE1011

ATOMIC NUMBER:                     2
NUMBER OF ELECTRONS:               2
MAGNETIC FIELD IN TESLA:           9.4021600E+07
PARTITION OF FINITE ELEMENTS:      2
NUMBER OF FINITE ELEMENTS:        15
UPPER INTEGRATION LIMIT:           8.0000000E+00
NUMBER OF CALCULATED STATES:       2
STATE 1
QUANTUM NUMBERS AND PARAMETER  1:  0 0 5.0000000E-01
QUANTUM NUMBERS AND PARAMETER  2:  1 0 5.0000000E-01
STATE 2
QUANTUM NUMBERS AND PARAMETER  1:  0 0 5.0000000E-01
QUANTUM NUMBERS AND PARAMETER  2:  1 1 1.0000000E+00

CALCULATION OF STATE 1, NAME = HE1011

ITERATION STEP  1:
ENERGY  1            -260.2037 eV
ENERGY  2            -146.6591 eV
TOTAL ENERGY         -535.1875 eV

ITERATION STEP  2:
ENERGY  1            -281.9497 eV
ENERGY  2            -156.9016 eV
TOTAL ENERGY         -563.5120 eV
ENERGY DIFF.           28.3245 eV

ITERATION STEP  3:
ENERGY  1            -280.9232 eV
ENERGY  2            -156.5361 eV
TOTAL ENERGY         -563.6378 eV
ENERGY DIFF.            0.1257 eV

ITERATION STEP  4:
ENERGY  1            -280.9809 eV
ENERGY  2            -156.5715 eV
TOTAL ENERGY         -563.6383 eV
ENERGY DIFF.            0.0006 eV
```

```
CONVERGENCE OF STATE HE1011                          -563.6383 eV
============================================================

CALCULATION OF STATE 2, NAME = HE1011-2ND

ITERATION STEP  1:
ENERGY  1            -362.0145 eV
ENERGY  2             -11.5971 eV
TOTAL ENERGY         -400.1254 eV

ITERATION STEP  2:
ENERGY  1            -383.4217 eV
ENERGY  2             -11.9894 eV
TOTAL ENERGY         -418.6248 eV
ENERGY DIFF.           18.4993 eV

ITERATION STEP  3:
ENERGY  1            -383.4953 eV
ENERGY  2             -11.8891 eV
TOTAL ENERGY         -419.6975 eV
ENERGY DIFF.            1.0727 eV

ITERATION STEP  4:
ENERGY  1            -383.6492 eV
ENERGY  2             -11.8807 eV
TOTAL ENERGY         -419.7022 eV
ENERGY DIFF.            0.0047 eV

ITERATION STEP  5:
ENERGY  1            -383.6624 eV
ENERGY  2             -11.8805 eV
TOTAL ENERGY         -419.7022 eV
ENERGY DIFF.            0.0000 eV

CONVERGENCE OF STATE HE1011-2ND                      -419.7022 eV
============================================================

TRANSITION: DELTA M=0

OSCILLATOR STRENGTH                                   0.2381528
============================================================

FINALIZING HFFEM: 2008-02-06 15:43:23.493 +0100
```

TEST RUN OUTPUT OF C1011.INI

```
STARTING HFFEM IN  6 MPI PROCESSES: 2008-02-07 15:11:19.464 +0100

PARAMETERS OF JOB C1011

ATOMIC NUMBER:                     6
NUMBER OF ELECTRONS:               6
MAGNETIC FIELD IN TESLA:           2.3505400E+08
PARTITION OF FINITE ELEMENTS:      2
NUMBER OF FINITE ELEMENTS:        18
UPPER INTEGRATION LIMIT:           1.0000000E+01
NUMBER OF CALCULATED STATES:       2
STATE 1
QUANTUM NUMBERS AND PARAMETER  1:  0 0 1.6666667E-01
QUANTUM NUMBERS AND PARAMETER  2:  1 0 1.6666667E-01
QUANTUM NUMBERS AND PARAMETER  3:  2 0 1.6666667E-01
QUANTUM NUMBERS AND PARAMETER  4:  3 0 1.6666667E-01
QUANTUM NUMBERS AND PARAMETER  5:  4 0 1.6666667E-01
QUANTUM NUMBERS AND PARAMETER  6:  5 0 1.6666667E-01
STATE 2
QUANTUM NUMBERS AND PARAMETER  1:  0 0 1.6666667E-01
QUANTUM NUMBERS AND PARAMETER  2:  1 1 1.0000000E+00
QUANTUM NUMBERS AND PARAMETER  3:  2 0 1.6666667E-01
QUANTUM NUMBERS AND PARAMETER  4:  3 0 1.6666667E-01
QUANTUM NUMBERS AND PARAMETER  5:  4 0 1.6666667E-01
QUANTUM NUMBERS AND PARAMETER  6:  5 0 1.6666667E-01

CALCULATION OF STATE 1, NAME = C1011

ITERATION STEP  1:
ENERGY  1           -1282.7005 eV
ENERGY  2            -644.9057 eV
ENERGY  3            -432.6637 eV
ENERGY  4            -325.7419 eV
ENERGY  5            -256.6350 eV
ENERGY  6            -192.7489 eV
TOTAL ENERGY        -5615.9911 eV

ITERATION STEP  2:
ENERGY  1           -1373.7898 eV
ENERGY  2            -691.9030 eV
ENERGY  3            -465.4142 eV
ENERGY  4            -350.4575 eV
ENERGY  5            -275.8201 eV
```

```
ENERGY  6            -208.4627 eV
TOTAL ENERGY        -5840.1243 eV
ENERGY DIFF.          224.1331 eV

ITERATION STEP  3:
ENERGY  1           -1369.2195 eV
ENERGY  2            -688.5474 eV
ENERGY  3            -462.8097 eV
ENERGY  4            -348.3919 eV
ENERGY  5            -274.1247 eV
ENERGY  6            -207.0572 eV
TOTAL ENERGY        -5840.4711 eV
ENERGY DIFF.            0.3468 eV

ITERATION STEP  4:
ENERGY  1           -1369.9395 eV
ENERGY  2            -689.0924 eV
ENERGY  3            -463.2283 eV
ENERGY  4            -348.7144 eV
ENERGY  5            -274.3730 eV
ENERGY  6            -207.2586 eV
TOTAL ENERGY        -5840.4770 eV
ENERGY DIFF.            0.0059 eV

CONVERGENCE OF STATE C1011                        -5840.4770 eV
============================================================

CALCULATION OF STATE 2, NAME = C1011-2ND

ITERATION STEP  1:
ENERGY  1           -1483.1827 eV
ENERGY  2              -8.5330 eV
ENERGY  3            -577.0562 eV
ENERGY  4            -474.9226 eV
ENERGY  5            -397.0082 eV
ENERGY  6            -323.0346 eV
TOTAL ENERGY        -4979.6184 eV

ITERATION STEP  2:
ENERGY  1           -1565.8490 eV
ENERGY  2              -9.0633 eV
ENERGY  3            -609.2060 eV
ENERGY  4            -504.0594 eV
ENERGY  5            -422.8035 eV
ENERGY  6            -344.7891 eV
```

```
TOTAL ENERGY        -5170.0975 eV
ENERGY DIFF.          190.4791 eV

ITERATION STEP  3:
ENERGY  1           -1564.5919 eV
ENERGY  2              -9.7189 eV
ENERGY  3            -607.7201 eV
ENERGY  4            -502.5729 eV
ENERGY  5            -421.2407 eV
ENERGY  6            -343.1117 eV
TOTAL ENERGY        -5170.8144 eV
ENERGY DIFF.            0.7170 eV

ITERATION STEP  4:
ENERGY  1           -1562.4088 eV
ENERGY  2             -10.0340 eV
ENERGY  3            -605.5911 eV
ENERGY  4            -500.4397 eV
ENERGY  5            -419.1130 eV
ENERGY  6            -340.9827 eV
TOTAL ENERGY        -5171.1268 eV
ENERGY DIFF.            0.3124 eV

ITERATION STEP  5:
ENERGY  1           -1561.2863 eV
ENERGY  2             -10.0843 eV
ENERGY  3            -604.5084 eV
ENERGY  4            -499.3598 eV
ENERGY  5            -418.0438 eV
ENERGY  6            -339.9191 eV
TOTAL ENERGY        -5171.1744 eV
ENERGY DIFF.            0.0476 eV

CONVERGENCE OF STATE C1011-2ND                  -5171.1744 eV
============================================================

TRANSITION: DELTA M=0

OSCILLATOR STRENGTH                                0.0269415
============================================================

FINALIZING HFFEM: 2008-02-07 15:11:34.416 +0100
```

4 Acknowledgements

This work was supported by Deutsche Forschungsgemeinschaft within the SFB 382 "Methods and algorithms for simulating physical processes on high-performance computers" at the Universities of Tübingen and Stuttgart.

References

[1] Zampieri, L. et al., Astron. Astrophys. **378** (2001) L5.

[2] Sanwal, D., Pavlov, G. G., Zavlin, V. E., and Teter, A. A., Astrophys. J. **574** (2002) L61.

[3] Mereghetti, S. et al., Astrophys. J. **581** (2002) 1280.

[4] Haberl, F., Schwope, A. D., Hambaryan, V., Hasinger, G., and Motch, C., Astron. Astrophys. **403** (2003) L19.

[5] Haberl, F., Zavlin, V. E., Trümper, J., and Burwitz, V., Astron. Astrophys. **419** (2004) 1077.

[6] van Kerkwijk, M. H., Kaplan, D. L., Durant, D. L., Kulkarni, S. R., and Paerels, F., Astrophys. J. **608** (2004) 432.

[7] Ruder, H., Wunner, G., Herold, H., and Geyer, F., *Atoms in strong magnetic fields*, Springer, Heidelberg, 1994.

[8] Al-Hujaj, O. A. and Schmelcher, P., Phys. Rev. A **67** (2003) 023403.

[9] Al-Hujaj, O. A. and Schmelcher, P., Phys. Rev. A **68** (2003) 053403.

[10] Ivanov, M. V., J. Phys. B **27** (1998) 4513.

[11] Jordan, S., Schmelcher, P., Becken, W., and Schweizer, W., Astron. Astrophys. **335** (1998) L33.

[12] Becken, W., Schmelcher, P., and Diakonos, F. K., J. Phys. B **32** (1999) 1557.

[13] Lieb, E. H., Solovej, J. P., and Yngvason, J., Phys. Rev. Lett. **69** (1992) 749.

[14] Lieb, E. H., Solovej, J. P., and Yngvason, J., Commun. Pure Appl. Math. **47** (1994) 513.

[15] Lieb, E. H., Solovej, J. P., and Yngvason, J., Commun. Math. Phys. **16** (1994) 77.

[16] Lieb, E. H., Solovej, J. P., and Yngvason, J., Asymptotics of natural and artificial atoms in strong magnetic fields, in *The Stability of Matter: From Atoms to Stars, Selecta of E. H. Lieb*, edited by Thirring, W., pages 145–167, Springer, Heidelberg, 1997.

[17] Hilgenfeldt, S., Balder, S., and Zenger, C., Sparse grids: Applications to multi-dimensional schrödinger problems, Technical report, Technische Universität München, 1995.

[18] Garcke, J. and Griebel, M., J. Comp. Phys. **165** (2000) 694.

[19] Fritsche, L., Phys. Rev. B **33** (1986) 3976.

[20] Jones, P. B., Mon. Not. R. Astro. Soc. **216** (1985) 503.

[21] Kössl, D., Wolff, R. G., Müller, E., and Hillebrandt, W., Astron. Astrophys. **205** (1988) 347.

[22] Relovsky, B. M. and Ruder, H., Phys. Rev. A **53** (1996) 4068.

[23] Braun, M., Phys. Rev. A **65** (2002) 033415.

[24] Medin, Z. and Lai, D., Phys. Rev. A **74** (2006) 062507.

[25] Ackermann, J., Erdmann, B., and Roitzsch, R., J. Chem. Phys. **101** (1994) 7643.

[26] Ackermann, J. and Shertzer, J., Phys. Rev. A **54** (1996) 365.

[27] Braun, M., Schweizer, W., and Elster, H., Phys. Rev. A **57** (1998) 3739.

[28] Ram-Mohanans, L. R., Saigal, S., Dossa, D., and Shertzer, J., Comp. in Phys. **4** (1990) 50.

[29] Shertzer, J. and Levin, F. S., Phys. Rev. A **43** (1991) 2531.

[30] Light, J. C., Hamilton, I. P., and Lill, J. V., J. Chem. Phys. **82** (1985) 1400.

[31] Baye, D. and Heenen, P.-H., J. Phys. A **19** (1986) 2041.

[32] Baye, D. and Vincke, M., J. Phys. B **24** (1991) 3531.

[33] Melezhik, V. S., Phys. Rev. A **48** (1993) 4528.

[34] Schweizer, W. and Faßbinder, P., Comp. in Phys. **11** (1997) 641.

[35] Ivanov, M. V. and Schmelcher, P., Phys. Rev. A **57** (1998) 3793.

[36] Ivanov, M. V. and Schmelcher, P., Phys. Rev. A **60** (1999) 3558.

[37] Ivanov, M. V. and Schmelcher, P., Phys. Rev. A **61** (2000) 022505.

[38] Ivanov, M. V. and Schmelcher, P., J. Phys. B **34** (2001) 2031.

[39] Al-Hujaj, O. A. and Schmelcher, P., Phys. Rev. A **70** (2004) 033411.

[40] Al-Hujaj, O. A. and Schmelcher, P., Phys. Rev. A **70** (2004) 23411.

[41] Neuhauser, D., Langanke, K., and Koonin, S. E., Phys. Rev. A **33** (1986) 2084.

[42] Miller, M. C. and Neuhauser, D., Mon. Not. R. Astro. Soc. **253** (1991) 107.

[43] Rajagopal, M., Romani, R. W., and Miller, M. C., Astrophys. J. **479** (1997) 347.

[44] Jones, M. D., Ortiz, G., and Ceperley, D. M., Phys. Rev. A **54** (1996) 219.

[45] Mori, K. and Hailey, C. J., Astrophys. J. **564** (2002) 914.

[46] Mori, K., Chonko, J. C., and Hailey, C. J., Astrophys. J. **631** (2005) 1082.

[47] Mori, K. and Hailey, C. J., Astrophys. J. **648** (2006) 1139.

[48] Engel, D., *Hartree-Fock-Roothaan calculations for many-electron atoms in neutron-star magnetic fields*, PhD thesis, University of Stuttgart, 2008, : http://elib.uni-stuttgart.de/opus/volltexte/2008/3386/.

[49] Engel, D. and Wunner, G., Phys. Rev. A. (2008), accepted for publication.

[50] Bücheler, S., Engel, D., Main, J., and Wunner, G., Phys. Rev. A. **76** (2007) 032501.

[51] Klews, M., *Discretization Methods for the Investigation of Atoms in Time-Dependent Electric Fields and Extremely Strong Magnetic Fields*, PhD thesis, University of Tübingen, 2003, http://tobias-lib.ub.uni-tuebingen.de/volltexte/2003/1022/.

[52] de Boor, C., SIAM J. Numer. Anal. **14** (1977) 441.

[53] de Boor, C., *A practical guide to splines*, Springer, Heidelberg, 1978.

[54] Schiff, L. I. and Snyder, H., Phys. Rev. **55** (1937) 59.

[55] Canuto, V. and Ventura, J., Quantizing magnetic fields in astrophysics, in *Fundamentals of Cosmic Physics*, volume 2, pages 203–353, Gordon and Breach Science Publishers, New York, 1977.

[56] Zienkiewicz, O. C. and Taylor, R. L., *The Finite Element Method*, Elsevier Ltd, Oxford, 6th edition, 2005.

[57] Braess, D., *Finite Elements*, Cambridge University Press, Cambridge, 3rd edition, 2007.

[58] Canuto, V. and Kelly, D. C., Astrophys. Space Sci. **17** (1972) 277.

[59] Brent, W., *Algorithms for Minimisation Without Derivatives*, Prentice Hall, New Jersey, 1972.

[60] Zhang, S. and Jin, J., *Computation of Special Functions*, Wiley-Interscience, New Jersey, 1996.

[61] Sokolov, A. A. and Ternov, I. M., *Synchrotron Radiation*, Akademie-Verlag, Berlin, 1968.